



Published in final edited form as:

Gastroenterology. 2017 April ; 152(5): 1187–1202. doi:10.1053/j.gastro.2016.12.033.

Choline Kinase α Mediates Interactions Between the Epidermal Growth Factor Receptor and Mechanistic Target of Rapamycin Complex 2 in Hepatocellular Carcinoma Cells to Promote Drug Resistance and Xenograft Tumor Progression

Xi-Meng Lin^{1,2,*}, Liang Hu^{1,3,*}, Jin Gu^{4,*}, Ruo-Yu Wang^{2,*}, Liang Li^{1,5}, Jing Tang⁶, Bao-Hua Zhang², Xing-Zhou Yan², Yan-Jing Zhu^{1,5}, Cong-Li Hu¹, Wei-Ping Zhou², Shao Li⁷, Jing-Feng Liu⁸, Frank J. Gonzalez⁹, Meng-Chao Wu², Hong-Yang Wang^{1,5}, Lei Chen^{1,5,8,9}

¹International Co-operation Laboratory on Signal Transduction, Eastern Hepatobiliary Surgery Institute, Second Military Medical University, Shanghai, China; ²Department of Hepatic Surgery, Eastern Hepatobiliary Surgery Hospital, Shanghai, China; ³Anal-Colorectal Surgery Institute, 150th Hospital of PLA, Luoyang, China; ⁴Tsinghua National Laboratory for Information Science and Technology, Bioinformatics Division, Synthetic and Systems Biology Center, Department of Automation, Tsinghua University, Beijing, China; ⁵National Center for Liver Cancer, Shanghai, China; ⁶Department of Neurosurgery, Wuhan General Hospital of Guangzhou Command, Wuhan, China; ⁷MOE Key Laboratory of Bioinformatics and Bioinformatics Division, Tsinghua National Laboratory for Information Science and Technology, Department of Automation, Tsinghua University, Beijing, China; ⁸Mengchao Hepatobiliary Hospital, Fujian Medical University, Fuzhou, China; ⁹Laboratory of Metabolism, Center for Cancer Research, National Cancer Institute, National Institutes of Health, Bethesda, Maryland

Abstract

BACKGROUND & AIMS: Choline kinase α (CHKA) catalyzes conversion of choline to phosphocholine and can contribute to carcinogenesis. Little is known about the role of CHKA in the pathogenesis of hepatocellular carcinoma (HCC).

METHODS: We performed whole-exome and transcriptome sequence analyses of 9 paired HCC and non—tumor-adjacent tissues. We performed tissue chip analyses of 120 primary HCC and non—tumor-adjacent tissues from patients who received surgery in Shanghai, China from January 2006 through December 2009; 48 sets specimens (HCC and non—tumor-adjacent tissues) were

Reprint requests: Address requests for reprints to: Lei Chen, PhD, International Co-operation Laboratory on Signal Transduction, Eastern Hepatobiliary Surgery Institute, Second Military Medical University, 225 Changhai Road, Shanghai 200438, China. chenlei@smmu.edu.cn; fax: (86) 21 6556 6851. Hong-Yang Wang, PhD, MD, International Co-operation Laboratory on Signal Transduction, Eastern Hepatobiliary Surgery Institute, Second Military Medical University, 225 Changhai Road, Shanghai 200438, China. hywangk@vip.sina.com; fax: (86) 21 6556 6851.

* Authors share co-first authorship.

Conflicts of interest

The authors disclose no conflicts.

Supplementary Material

Note: To access the supplementary material accompanying this article, visit the online version of *Gastroenterology* at www.gastrojournal.org, and at <http://dx.doi.org/10.1053/j.gastro.2016.12.033>.

also analyzed. *CHKA* gene copy number was quantified and findings were validated by quantitative reverse transcription polymerase chain reaction analysis. *CHKA* messenger RNA and protein levels were determined by polymerase chain reaction, immunohisto-chemical, and immunoblot analyses. *CHKA* was examined in 2 hepatocyte cell lines and 7 HCC-derived cell lines, and knocked down with small interfering RNAs in 3 HCC cell lines. Cells were analyzed in proliferation, wound healing, migration, and invasion assays. Cells were injected into tail veins of mice and tumor growth and metastasis were quantified. Immunoprecipitation and immunofluorescence assays were conducted to determine interactions between *CHKA* and the epidermal growth factor receptor (EGFR) and the mechanistic target of rapamycin complex 2.

RESULTS: Levels of *CHKA* messenger RNA were frequently increased in HCC tissues compared with nontumortissues; increased expression was associated with amplification at the *CHKA* loci. Tumors that expressed high levels of *CHKA* had more aggressive phenotypes, and patients with these tumors had shorter survival times after surgery compared to patients whose tumors expressed low levels of *CHKA*. HCC cell lines that stably overexpressed *CHKA* had higher levels of migration and invasion than control HCC cells, and formed larger xenograft tumors with more metastases in mice compared to HCC cells that did not overexpress *CHKA*. *CHKA* was required for physical interaction between EGFR and mechanistic target of rapamycin complex 2. This complex was required for HCC cells to form metastatic xenograft tumors in mice and to become resistant to EGFR inhibitors.

CONCLUSIONS: We found levels of *CHKA* to be increased in human HCCs compared to nontumor tissues, and increased expression to be associated with tumor aggressiveness and reduced survival times of patients. Overexpression of *CHKA* in HCC cell lines increased their invasiveness, resistance to EGFR inhibitors, and ability to form metastatic tumors in mice by promoting interaction of EGFR with mechanistic target of rapamycin complex 2.

Keywords

Liver Cancer; Signal Transduction; Tumorigenesis; Oncogene

Liver cancer is one of the leading causes of cancer-related death worldwide and is particularly prevalent in China. According to data from the International Agency for Research on Cancer, there were an estimated 782,500 new cases of liver cancer and 745,500 deaths during 2012, with China alone accounting for about 50% of the total number of cases and deaths.¹ Among the primary liver cancers, hepatocellular carcinoma (HCC) represents the major histologic subtype. Despite recent advancements in the diagnosis and treatment approaches, the prognosis for HCC patients remains dismal due to postsurgical recurrence and distant metastasis.² Great efforts have been made to explore the mechanism underlying the pathogenesis of HCC during the past decades; however, the detailed molecular events contributing to HCC progression and metastasis are still not fully understood.³ Therefore, there remains an urgent need to search for novel prognostic biomarkers and therapeutic targets for HCC therapy.^{4,5}

Epidermal growth factor receptor (EGFR) has been documented to be overexpressed in around 40 % –70 % of human HCCs.⁶ Elevated expression of the EGFR ligands has also been reported in the preneoplastic lesions of liver tissues, indicating its potential role in

hepatocarcinogenesis. Although EGFR antagonists have an effect on cell malignancy in human HCC cells and in animal HCC model, several clinical trials was unable to show significant survival improvement with gefitinib, cetuximab,⁷ or erlotinib⁸ in HCC patients. These data reinforced the importance of better understanding the mechanisms and identifying potential intracellular effectors whereby EGFR signaling influences HCC progression.

Choline kinase, the first enzyme in the Kennedy pathway that catalyzes the phosphorylation of free choline to phosphocholine, is responsible for de novo biosynthesis of phosphatidylcholine.^{9,10} Activated choline phospholipid metabolism has been implicated in oncogenesis and progression and been proposed as a metabolic hallmark of cancer.^{9,11–17} Until now, accumulating evidence has supported the oncogenic property of CHKA in cancer pathobiology apart from its metabolic function,^{9,15,18–20} In addition, the diagnostic and prognostic significance of CHKA expression in human malignant diseases has also been revealed.²¹ Recently, it has been documented that co-overexpression of both EGFR and c-Src increased CHKA protein levels,²² but whether the abnormal expression of CHKA was involved in EGFR signal activity and its potential role for HCC progression have not been explored until now.

To address these issues, expression patterns of CHKA in HCC and its clinicopathologic significance in a HCC cohort were investigated first. In addition, its contribution to the progression and metastasis of HCC, both in vitro and in vivo, was examined and the underlying relationship with EGFR-related signal pathway was further dissected. The current results provide novel mechanistic insights into a critical role of CHKA in EGFR—mechanistic target of rapamycin complex 2 (mTORC2) activity in HCC metastasis and therapeutic resistance, suggesting a potential prognostic marker and synergetic target for EGFR-dependent tumor, together with commercial anti-EGFR drugs gefitinib or erlotinib.

Methods

Patients and Samples

Nine paired HCC and non—tumor-adjacent tissues were used for next-generation sequencing technology carrying out whole-exome and transcriptome sequencing to identify copy number variation. Specimens, including 120 primary HCC and non—tumor-adjacent tissues from HCC patients who received curative surgery in the Eastern Hepatobiliary Surgery Hospital (Shanghai, China) from January 2006 to December 2009, were used for tissue microarray. Forty-eight sets of HCC specimens (HCC and non—tumor adjacent tissues) were used for quantitative real-time polymerase chain reaction (qRT-PCR) or Western blot analysis. Written informed consent was obtained from each patient and these studies were approved by the Ethics Boards of the Eastern Hepatobiliary Surgery Hospital.

Cell Cultures, Stable Cell Line Construction, and RNA Interfering

The normal-type hepatocyte QSG7701 and HL7702 cells, as well as the HCC cell lines Huh-7, SNU-475, HepG2, Hep3B, PLC/PRF/5, SMC7721, MHCC-97L, and MHCC-97H, were purchased from the Shanghai Cell Bank of the Chinese Academy of Sciences

(Shanghai, China). Cells were maintained at 37°C in an atmosphere containing 5% CO₂ in Dulbecco's modified Eagle medium supplemented with 10% fetal bovine serum. Lentivirus productions for stable cell line construction were completed by the Genechem Company (Shanghai, China) and used according to the manufacturer's instructions. For RNA interfering, cells were transfected with 100 nM small interfering (si)RNAs by INTERFERin transfection reagent (409–10; Polyplus, New York, NY) according to manufacturer's instructions. siRNAs were purchased from the Biotend Company (Shanghai, China). For more information, see the Supplementary Methods.

Animal Studies

All animal experiments were performed in accordance with the guidelines for the care and use of laboratory animals and were approved by the Ethics Boards of the Eastern Hepatobiliary Surgery Hospital. For in vivo metastasis assays, cells were injected into the caudal veins of 5-week-old male BALB/C nude mice. Each group had 5 mice. All of the mouse groups were killed after 8 weeks. The lungs of each mouse were separated and fixed for H&E staining. The mean number of metastatic foci in each group was counted under a microscope. For xenografts and in vivo drug studies, cells were injected subcutaneously into the right posterior flanks of 6-week-old female BALB/C nude mice. When the tumor reached a volume of approximately 100 mm³ in size, mice were randomized into indicated groups (n = 6) and subjected to treatment with vehicle or erlotinib (80 mg/kg/d) orally. Tumor growth was measured every 5 days for a total period of 35–40 days. Tumor volume = 1/2 length × (width)². At day 40, mice were sacrificed and tumors were photographed. H&E, immunohistochemistry, and terminal deoxynucleotidyl transferase-mediated deoxyuridine triphosphate nick-end labeling staining were performed on paraffin-embedded specimens of xenograft tumors. For more information, see Supplementary Methods.

Statistical Analysis

All of the measurement data are expressed as mean ± SD. Pearson χ^2 test was used to analyze the relationships between the expression of CHKA and the clinicopathologic features. A Kaplan-Meier analysis was used to assess the differences in survival rates. SPSS software, version 16.0 (SPSS Inc, Chicago, IL) was used for the statistical analyses. $P < .05$ was considered to be statistically significant.

All authors had access to the study data and reviewed and approved the final manuscript. For more materials and methods, see Supplementary Methods.

Results

Increased Choline Kinase α Expression Correlates With Aggressive Clinicopathologic Features and Predicts Poor Prognosis in Hepatocellular Carcinoma Patients

To elucidate functional genomic aberrations underlying human HCC, the genomic disorder screening method, including targeted capture; massively parallel paired-end sequencing; and whole transcriptome sequencing technologies, were employed on 9-paired HCC samples including tumor and their counterpart non-tumor-adjacent tissues. As shown in Supplementary Figure 1A and B, the abnormal amplification region spanning 11q13.2–13.3

(covering up to 24 genes) were uncovered and verified by qRT-PCR. Then, the public HCC databases (GSE22058, GSE25097, GSE36376, GSE46444, GSE54236, GSE63898, and TCGA, detailed see in Supplementary Table 1) and CIPHER ranking method²³ were consulted to confirm the different genes spanning the 11q13.2–13.3 region, among which 7 genes, including *PPFIA1*, *LRP5*, *CCND1*, *MYEOV*, *CHKA*, *NDUSF8*, and *ORAOV1* were found to be frequently up-regulated in HCC tumor tissues (Figure 1A and Supplementary Tables 2 and 3). To further verify the potential contribution of genomic disorder to tumor progression, siRNA-mediated gene knockdown was used to screen these 7 genes (Supplementary Figure 1E) in 2 immortal cell lines, Huh-7 and SNU-475, both possessing an amplified genomic 11q13.2–13.3 region (Supplementary Figure 1F and G). Interestingly, among those genes, only down-regulation of *CHKA* was found to significantly inhibit cell motility in both cell lines without affecting cell proliferation (Supplementary Figure 1C and D). As expected, qRT-PCR, Western blot, and immunohistochemistry methods further revealed the similar expression trend of *CHKA* within our clinical HCC samples (Figure 1B–D and Supplementary Figure 2A), and the positive correlation between *CHKA* gene copy number and messenger RNA expression level (Supplementary Figure 2B; $P = .0001$).

Further analysis revealed the relationship between higher *CHKA* expression and several aggressive clinicopathologic features, including positive microvascular invasion, advanced Barcelona Clinic liver cancer (BCLC) stage, early disease recurrence, and patient death (Supplementary Table 4 and Figure 1E). Multivariate Cox regression analysis demonstrated that increased *CHKA* expression ($P = .003$) and microvascular invasion ($P = .001$) were independently associated with poor overall survival, while high *CHKA* expression ($P = .007$), together with tumor size ($P = .035$) and microvascular invasion ($P < .001$), was also an independent predictor of cancer recurrence in patients with HCC (Figure 1F). Together, these data indicate that *CHKA* expression is frequently up-regulated in human HCC tissues, at least partly resulting from genomic amplification, and correlates with malignant progression and unfavorable prognosis of HCC.

Choline Kinase α Enhances Invasion and Metastasis of Hepatocellular Cells in vitro and in vivo

Given the significant correlation between *CHKA* expression level and aggressive tumor characteristics, we hypothesize that *CHKA* plays a functional role in HCC progression. We examined *CHKA* expression in 9 liver cell lines, including 2 normal hepatocyte cell line (HL7702 and QSG7701), 7 HCC-derived cell lines (HepG2, Huh-7, Hep3B, PLC/PRF/5, SMMC7721, MHCC-97L, and MHCC-97H). Consistent with the findings in HCC tissue samples, both qRT-PCR and Western blot assays revealed that *CHKA* expression level was higher in HCC-derived cell lines than in normal liver cell lines (Supplementary Figure 3A and B). GFP-tagged *CHKA*-expressing recombinant lentivirus (LV-*CHKA*) was used to establish *CHKA* stable cell lines in HL7702 and SMMC7721, which have low levels of endogenous *CHKA* (Figure 2A). Although no substantial difference in proliferation rate was observed between *CHKA*-overexpressed and control cells (Supplementary Figure 3C), scratch wound healing, Transwell migration, and Matrigel invasion assays clearly demonstrated that forced expression of *CHKA* markedly enhanced the migratory and invasive abilities of both HL7702 and SMMC7721 cells (Figure 2B and C and

Supplementary Figure 3D and E). In addition, LV-CHKA-or *LVV-GFP*—infected SMMC7721 cells were injected into the lateral tail vein of nude mice to determine the extent of lung metastasis. Eight weeks later, more and larger micrometastatic lesions were observed microscopically in lungs from mice injected with LV-CHKA-SMMC7721 cells compared with those with LV-GFP cells (Figure 2D).

In addition, we depleted CHKA expression via siRNA in 3 HCC cell lines, LV-*CHKA*—infected SMMC7721, Huh-7 and MHCC-97H (Supplementary Figure 3F). No significant reduction in cell proliferation was noted in *CHKA*-silenced cells (Supplementary Figure 3G), whereas CHKA knockdown greatly impaired the migration and invasion capabilities of each cell line (Figure 2E and Supplementary Figure 3H and I). In addition, lung metastasis was also determined using short-hairpin (sh)*CHKA*- or sh-negative control (NC)-huh7 cells (Supplementary Figure 3J), with results that less and smaller micrometastatic lesions were observed microscopically in lungs from nude mice injected with sh*CHKA*-huh7 cells compared with those with shNC cells, 8 weeks after tail vein injection (Figure 2F). Collectively, these findings support the view that CHKA positively regulates the invasiveness and metastatic potential of HCC cells both in vitro and in vivo.

Choline Kinase α Facilitates Hepatocellular Carcinoma Metastasis Through Activating AKT Signaling

Consistent with a previous finding showing that CHKA regulates v-akt murine thymoma viral oncogene homolog (AKT) activity,²⁴ phosphorylated AKT (p-AKT) was observed in both CHKA-overexpressed HL7702 and SMMC7721 cells; conversely, specific knockdown of *CHKA* by siRNA markedly suppressed AKT phosphorylation in all 3 CHKA-expressing cell lines (Figure 2G). Inhibition of extra-cellular regulated kinase (ERK) phosphorylation in the absence of *CHKA* was also observed, in agreement with previous reports²⁵ (Supplementary Figure 4A). We then tested whether the AKT or ERK signaling pathway is required for CHKA-mediated HCC metastasis. As illustrated in Supplementary Figure 4B–D, specific inhibition of AKT activity by either of its pharmacologic inhibitors, M K2206 or AZD5363, substantially impaired the migration and invasion capabilities of CHKA-overexpressed SMMC7721 and Huh-7 cells. However, the MEK1/ERK inhibitors (PD 98059 and U 0126) also effectively blocked the ERK activity, but showed no effect on cell motility (Supplementary Figure 4E and F), indicating that AKT-dependent signaling, rather than the mitogen-activated protein kinase signal pathway, plays a major role in CHKA-enhanced HCC metastasis. To rule out the possible off-target effects emanating from AKT pharmacologic inhibitors, siRNA-mediated *AKT1* silencing experiments were performed. Consistently, AKT1 depletion vigorously suppressed the migratory and invasive properties of HCC cell lines expressing high levels of exogenous or endogenous CHKA (Figure 2H and Supplementary Figure 4G). Furthermore, we observed that activation of AKT signaling by ectopic expression of myr-AKT, the constitutively active form of AKT, significantly restored the migratory and invasive capabilities after si*CHKA* treatment (Figure 2I and Supplementary Figure 4H). Taken together, these results suggest that CHKA promotes HCC cell metastasis mainly via activation of AKT signaling.

We further analyzed the expression levels of CHKA and p-AKT in 7 HCC cell lines and clinical HCC samples. Western blot analysis of HCC cell lines and tissue microarray analysis of HCC specimens from 120 patients revealed a close correlation of CHKA expression with p-AKT levels, which further supports the activation of AKT by CHKA in HCC cell lines (Supplementary Figure 4I) and clinical HCC tissues (Figure 2J). Growing evidence has indicated that a combination of multiple markers might be more informative than any single marker for the prediction of clinical outcomes of patients with HCC. We then evaluated whether the combination of the 2 parameters could increase the efficiency in prognosis prediction. Indeed, patients whose tumors have both elevated CHKA and enhanced p-AKT levels showed the worst prognosis, indicating that the combination of the 2 parameters provides an improved prognostic value in comparison with either CHKA or p-AKT alone (Figure 2K and Supplementary Table 5).

Choline Kinase α Physically Interacts With Epidermal Growth Factor Receptor, Promotes Epidermal Growth Factor Receptor Autophosphorylation and Dimerization on Plasma Membrane

We then investigated which upstream regulator²⁶ is necessary for the enhanced AKT activation and HCC metastasis induced by CHKA. Interestingly, upon EGF stimulation, overexpression of CHKA robustly enhanced AKT activation, while knockdown of its expression by siRNA markedly suppressed AKT activation. However, no such changes were observed in response to hepatocyte growth factor stimulation (Figure 3A and Supplementary Figure 5), implying that EGFR, but not c-Met, may be involved in mediating the effects of CHKA. In addition, after EGF stimulation, the phosphorylation levels of 3 residues (Y992, Y 1045, and Y 1068) in EGFR were significantly increased after forced CHKA expression, while greatly decreased in CHKA-depleted cells, paralleled with the changes of p-AKT (Figure 3B). Cell surface expression of EGFR, the EGF-induced receptor dimerization, or endocytosis was also examined in the presence of CHKA. At baseline, a higher percentage of membrane EGFR-positive cells was observed in the CHKA-overexpressed cells compared with control cells (81% vs 64%). After stimulation with EGF, CHKA-overexpressed cells exhibited a slower EGFR internalization than control cells. On the contrary, CHKA-depleted cells exerted the opposite effects (Figure 3C). In addition, cross-linking experiments²⁷ were performed to examine the effects of CHKA on EGF-induced dimerization of EGFR, and we found that forced expression of CHKA increased EGF-induced EGFR dimerization, whereas CHKA silencing did the opposite (Figure 3D). We then investigated whether CHKA and EGFR could physically interact by performing co-immunoprecipitation experiments in cells expressing CHKA. Interestingly, an interaction between EGFR and exogenous or endogenous CHKA was observed in reciprocal co-immunoprecipitation assays (Figure 3E). Consistently, evidence of membrane colocalization (*yellow*: merged CHKA [*green*] and EGFR [*red dots*]) was observed via immunofluorescence confocal microscopy (Figure 3F). In addition, confocal-based immunofluorescence imaging also revealed a delayed internalization of EGFR into the cytoplasm in CHKA-overexpressed SMMC7721 cells, or an accelerated internalization of EGFR into the cytoplasm in CHKA-depleted Huh-7 cells, upon EGF stimulation. Collectively, these results indicate that CHKA may exert its pro-metastatic properties through binding with EGFR, promoting EGFR dimerization, while preventing EGFR internalization, thereby enhancing EGFR-AKT activation.

Epidermal Growth Factor Receptor—Mechanistic Target of Rapamycin Complex 2 Axis Is Indispensable for Choline Kinase α —Enhanced AKT Activation and Hepatocellular Carcinoma Metastasis

In the additional studies, specific knockdown of EGFR expression by siRNA completely abrogated the effects of CHKA on both EGFR and AKT phosphorylation on EGF stimulation (Figure 4A). In addition, similar results were also obtained independent of EGF stimulation, together with the complete elimination of the differences in the migratory and invasive properties between CHKA-overexpressed or CHKA-depleted cells and their control counterparts (Figure 4B and Supplementary Figure 6), proving an essential role in CHKA-induced AKT activation and HCC metastasis.

To determine the downstream mechanism by which EGFR mediates the effects of CHKA on AKT activation and HCC metastasis, we assessed the possible involvement of several well-characterized regulators of AKT phosphorylation, including phosphoinositide 3-kinase (PI3K), phosphoinositide-dependent kinase-1, and mTORC2. Notably, the phosphorylated levels of P85 (p-P85) were increased in CHKA-overexpressed cells and decreased in CHKA-depleted cells, and EGFR siRNA knockdown also blocked the effects of CHKA on p-P85 upon EGF stimulation (Supplementary Figure 7A and B). Nevertheless, inhibition of PI3K activity by its pharmacologic inhibitor LY294002, which effectively suppressed p-P85 and p-AKT (Thr308) levels in each cell line, failed to attenuate the difference of p-AKT (ser473) and HCC cell metastatic potential between CHKA-overexpressed or CHKA-depleted cells and control cells (Supplementary Figure 7C and D). This finding was in agreement with a previous study reporting that CHKA regulation on AKT activity is PI3K independent,²⁴ indicating that PI3K is not indispensable for CHKA-facilitated AKT (ser473) phosphorylation and metastasis. In addition, knockdown of phosphoinositide-dependent kinase-1 by siRNA, which completely blocked the CHKA-mediated AKT (Thr308) activation, also failed to affect CHKA-triggered AKT (Ser473) phosphorylation and HCC cell metastatic phenotype (Supplementary Figure 8), suggesting that neither phosphoinositide-dependent kinase-1 nor AKT (Thr308) activation plays an essential role in CHKA-induced HCC metastasis.

Interestingly, siRNA-mediated knockdown of RPTOR independent companion of mTOR complex 2 (*RICTOR*), the core component of mTORC2 responsible for AKT (Ser473) phosphorylation,²⁸ clearly abrogated the distinct activation of AKT (Ser473) between CHKA-overexpressed or CHKA-silenced cells and their counterparts. Meanwhile, no changes were observed in the phosphorylation levels of EGFR when *RICTOR* was silenced (Figure 4C and D). In addition, *RICTOR* knockdown also completely abolished CHKA-enhanced cell migration and invasion (Figure 4D and Supplementary Figure 9A). Similarly, pharmacologic inhibition of mTOR kinase activity by mTORC1/C2 inhibitor PP242²⁹ completely blocked CHKA-enhanced AKT (ser473) phosphorylation and tumor cell metastasis. However, treatment of cells with mTORC1 inhibitor rapamycin failed to disturb the effects of CHKA (Figure 4E and F and Supplementary Figure 9B). Together, these results reveal that the EGFR—mTORC2 axis is necessary for CHKA-dependent AKT (ser473) activation and HCC metastasis.

Overexpression of Choline Kinase α Facilitates Functional Interaction Between Epidermal Growth Factor and mTOR Complex 2 By Acting as an Adaptor Protein

Given our findings that CHKA-EGFR interaction and the presence of mTORC2 is necessary for CHKA function, we hypothesize that CHKA may serve as a mediator to promote the association of EGFR with mTORC2. Importantly, the pairwise interactions of RICTOR, EGFR, and CHKA were observed in CHKA-overexpressed SMMC7721 cells, together with an enhanced mTORC2 kinase activity (Figure 5A). The interaction of RICTOR, EGFR, and endogenous CHKA was also observed in Huh-7 cells, and was remarkably ameliorated after CHKA was silenced, which also impaired mTORC2 kinase activity, indicating that CHKA is necessary for EGFR—RICTOR interaction (Figure 5B). In addition, immunofluorescence confocal imaging also confirmed the membrane colocalization (*white*) of CHKA (*green*), EGFR (*red*), and RICTOR (*blue*) in CHKA-overexpressed SMMC7721 cells and Huh-7 cells (Figure 5C and D). However, the membrane colocalization (*white*) of endogenous CHKA (*green*), RICTOR (*blue*), and EGFR (*red*) was barely detectable in CHKA-silenced cells as compared to their control counterparts (Figure 5D). Furthermore, we employed 4 HCC cell lines, including SMMC7721 and PLC/PRF/5 cells, which express lower levels of endogenous CHKA, and Huh-7 and MHCC-97H cells, which express higher levels of endogenous CHKA, and performed co-immunoprecipitation assays and confocal-based immunofluorescence imaging to evaluate whether CHKA expression is responsible for the assembly of EGFR—RICTOR in these cell lines. As shown in Supplementary Figure 10, no obvious interaction or membrane colocalization of RICTOR and EGFR was observed in SMMC7721 and PLC/PRF/5 cells. By contrast, protein—protein interaction as well as membrane colocalization of RICTOR and EGFR was seen in both Huh-7 and MHCC-97H cells, supporting that protein levels of CHKA in the cell lines examined were associated with the assembly of EGFR-RICTOR complex. Collectively, these findings suggest that overexpression of CHKA protein in HCC cells may act as an adaptor molecule that facilitates functional interaction between EGFR and mTORC2, which is indispensable for CHKA-provoked AKT activation and HCC metastasis subsequently.

Overexpression of Choline Kinase α Promotes Resistance to Epidermal Growth Factor Receptor—Targeted Drugs in Hepatocellular Carcinoma

We then speculated whether dysregulated CHKA has a potential effect on EGFR-targeted therapies, 2 commercial small-molecule kinase inhibitors of EGFR,³⁰ gefitinib and erlotinib, were applied with CHKA-overexpressed and CHKA-silenced cells lines. As shown in Figure 6A–C and Supplementary Figure 11A and B, both short-term growth-inhibition and long-term colony-formation assays revealed that CHKA-overexpressed cells were more resistant to gefitinib and erlotinib treatment in comparison with control cells. Meanwhile, siRNA-mediated knockdown of RICTOR clearly abrogated the distinct sensitivity to the drugs between CHKA-overexpressed or CHKA-silenced cells. In addition, CHKA-overexpressed cells showed more resistant to the effects of gefitinib and erlotinib on cell migration and invasion. Conversely, gefitinib or erlotinib treatment combined with CHKA knockdown exhibited a synergetic inhibitory effect on cell metastasis (Supplementary Figure 11C). As expected, overexpression of CHKA rendered HCC cells more resistant to gefitinib and erlotinib-induced apoptosis, as indicated by diminished cleaved poly ADP-ribose polymerase. Invariably, silencing of *R/CTOR* again eliminated these differences (Figure

6D). In addition, we used immunodeficient mice xenografted with *LV-CHKA*— or *LV-GFP*—infected SMMC7721 tumors. Ten days after injection of tumor cells, palpable tumors were present in all animals, and cohorts of mice were treated with vehicle or erlotinib. As shown in Figure 6E, treatment of mice with erlotinib only resulted in marginal growth inhibition on CHKA-overexpressed SMMC7721 tumors. In contrast, it elicited a potent growth inhibition on tumors of the control group (Figure 6E), with an impaired level of p-AKT and apparent cell apoptosis, as indicated by terminal deoxynucleotidyl transferase-mediated deoxyuridine triphosphate nick-end labeling (Figure 6F). Because no alteration of p53 status or *K-RAS* gene mutation were observed among the cell lines we used (Supplementary Figure 11D and E), these results confirmed that CHKA could promote resistance to EGFR-targeted drugs both in vitro and in vivo, and also suggest the potential effectiveness of a dual inhibition of CHKA/mTORC2 to overcome the resistance of HCC cells to EGFR-targeted therapies.

Discussion

In the present work, we found that CHKA was commonly overexpressed in human HCCs, which may be, at least partially, due to amplification of its gene copy number. Up-regulated expression of CHKA was related to microvascular invasion, advanced tumor stage, early disease recurrence, and poor survival, and was an independent unfavorable prognostic indicator for HCC patients. In addition, CHKA promoted HCC invasion and metastasis through activation of EGFR-mTORC2-AKT signaling. Mechanistically, overexpression of CHKA interacted with EGFR and induced EGFR activation. Meanwhile, CHKA acted as an adaptor molecule facilitating functional interaction between EGFR and mTORC2, enhancing down-stream AKT signal and cancer metastasis. Furthermore, overexpression of CHKA also conferred resistance to anti-EGFR drugs gefitinib and erlotinib via promoting the formation of EGFR/mTORC2 (RICTOR) complex. To our knowledge, this is the first study that intensively evaluates the biologic relevance of CHKA in the progression and drug resistance of HCC.

Aberrant expression of CHKA was reported previously in HCC tissues. In a genomic profiling study, *CHKA* was identified as one of the up-regulated genes in a 73-gene expression signature associated with vascular invasion in HCC.³¹ Consistent with this finding, data from our qRT-PCR, Western blot, and immunohistochemistry assays confirmed the significant up-regulation of CHKA expression in HCC tissues and HCC-derived cell lines. In an attempt to explore the molecular basis for CHKA overexpression in HCC, we noticed that the *CHKA* gene is located at chromosome locus 11q13.3, one of the most frequent genomic amplification regions reported in various types of human cancers, including HCC,³² and hypothesized that elevated expression of CHKA in HCC may result from its gene copy number variation. As expected, relative DNA copy number of *CHKA* was positively correlated with its mRNA expression level, supporting a causal relationship between its gene amplification and up-regulated expression in HCC. Although several mechanisms for transcriptional induction of CHKA have been revealed,^{19,22,33–38} our current results cannot rule out the possible involvement of those mechanisms contributing to CHKA overexpression in HCC. Nevertheless, the observed amplification of *CHKA* gene may, at least in part, account for the up-regulation of CHKA in HCC.

Indeed, our gain-of-function and loss-of-function experiments clearly suggested a metastasis-promoting role of CHKA in HCC. To date, although the involvement of CHKA in cancer invasion and metastasis has been documented in several human malignancies, their underlying mechanism is still unclear. We found that ectopic expression of CHKA enhanced AKT phosphorylation. Administration of a specific pharmacologic inhibitor targeting AKT, siRNA-mediated AKT silencing, and over-expression experiments further verified the key role of AKT in CHKA-mediated HCC metastasis. A combination of CHKA and p-AKT also provided improved prognostic value for HCC.

In this study, we found that CHKA facilitates invasion and metastasis of HCC cells but has no effect on cell proliferation. The pro-invasive effect of CHKA is mainly through its activation of AKT signaling. Our results are in agreement with similar cases reported recently in which cancer-related genes^{39,40} either promote or suppress tumor invasion and metastasis by modulating AKT signaling, and have no major effect on cellular proliferation. Interestingly, when the HCC cells were cultured in low serum condition (2 % serum) instead of normal culture condition (10 % serum), a pro-proliferative effect of CHKA was observed (Supplementary Figure 12A). In addition, we also found the higher levels of p-AKT in CHKA-expressing cells than those in control cells under low serum culture circumstance (Supplementary Figure 12B). In comparison with the level under normal culture condition, the overall level of p-AKT is relatively lower in 2% serum culture medium. Also, we observed a pro-proliferative effect of CHKA in our xenograft tumor model in vivo (Figure 6E and F). Based on these observations, we speculate that, under normal culture conditions, the basal activity of p-AKT is enough to promote cell proliferation in either control or CHKA-overexpressed cells, thus higher level of p-AKT induced by CHKA may mainly contribute to cell metastasis and invasion. Under low serum culture condition, the activated p-AKT by CHKA will mainly contribute to cell proliferation. Further studies should be conducted to explore the underlying mechanism by which different levels of p-AKT facilitate cancer metastasis or cell proliferation in vivo.

Furthermore, we demonstrated that the interaction between CHKA and EGFR promoted the EGF-induced dimerization of EGFR, prevented the EGF-induced internalization of EGFR, and was necessary for CHKA-AKT signaling. More importantly, we found that overexpression of CHKA promoted the interactions among CHKA, EGFR, and RICTOR, the core component of mTORC2, and knockdown of CHKA profoundly impaired the interaction between EGFR and RICTOR. These findings indicate that CHKA may act as a functional adaptor molecule integrating EGFR and mTORC2, which is indispensable for AKT activation and cancer metastasis (Figure 7). It is currently unknown whether the interaction between the CHKA and mTORC2 is direct or indirect and, if it is direct binding, which domain of CHKA is essential for this binding. Further mechanistic analyses will be required to address this issue. Based on the findings that specific knockdown of CHKA attenuated the EGF-induced EGFR phosphorylation and no such effect was observed with siR/CTOR treatment, we conclude that the interaction of CHKA and EGFR is a prerequisite for the formation of EGFR/CHKA/RICTOR complex and EGFR/CHKA-induced mTORC2 activity. As our results showed that treatment of cells with CK37,⁴¹ a small molecule antagonist of CHKA, completely blocked the production of phosphatidylcholine and phosphatidic acid²⁵ in CHKA-overexpressed cells (Supplementary Figure 13A), but failed to

abrogate the enhanced AKT (Ser473) activation and pro-invasive property conferred by CHKA expression (Supplementary Figure 13B and C), these findings further support the notion that the CHKA protein itself, rather than its catalytic role, is more important in promoting cancer development and progression.⁴²

We also found a dramatically enhanced and continued EGF-induced EGFR signal activation in the presence of CHKA, which further confirmed that dysregulated expression of CHKA may synergistically strengthen EGFR signaling in HCC and contribute to the resistance of those tumors to EGFR targeted therapy. Importantly, knockdown of RICTOR completely abrogated CHKA-induced resistance to anti-EGFR drugs gefitinib and erlotinib, and even enhanced cell sensitivity to the drugs. We suggest that this paradigm be applied as a candidate pharmaceutical target for EGFR-dependent tumor therapy together with commercial anti-EGFR drugs.

In conclusion, the present study revealed that abnormal expression of CHKA plays an indispensable role in the progression and metastasis of HCC through inducing dimerization of EGFR, physically facilitating the formation of EGFR/CHKA/mTORC2 protein complex and enhancing mTORC2-dependent AKT phosphorylation, which not only sheds new light on HCC metastasis and drug resistance, but also provides a potential target for EGFR-positive cancer prevention and treatment.

Supplementary Material

Refer to Web version on PubMed Central for supplementary material.

Acknowledgments

The authors acknowledge the members of the International Co-operation Laboratory on Signal Transduction, especially Dong-Ping Hu, Shan-HuaTang, Lin-Na Guo, Dan Cao, Dan-Dan Huang, LiangTang, Shan-NaHuangforexcellenttechnical assistance.

Funding

This work was supported by the State Key Project for Liver Cancer (2012ZX10002-009), National Natural Science Foundation of China (81301811, 81521091, 81422032, 81272212, 81672860, 81372674, 91229201, and 91529303), Science Foundation of Shanghai (134119a3700), and Strategic Priority Research Program of the Chinese Academy of Sciences (XDA12010201).

Abbreviations used in this paper:

AKT	v-akt murine thymoma viral oncogene homolog
CHKA	choline kinase α
EGFR	epidermal growth factor receptor
ERK	extracellular regulated kinase
GFP	green fluorescent protein
HCC	hepatocellular carcinoma

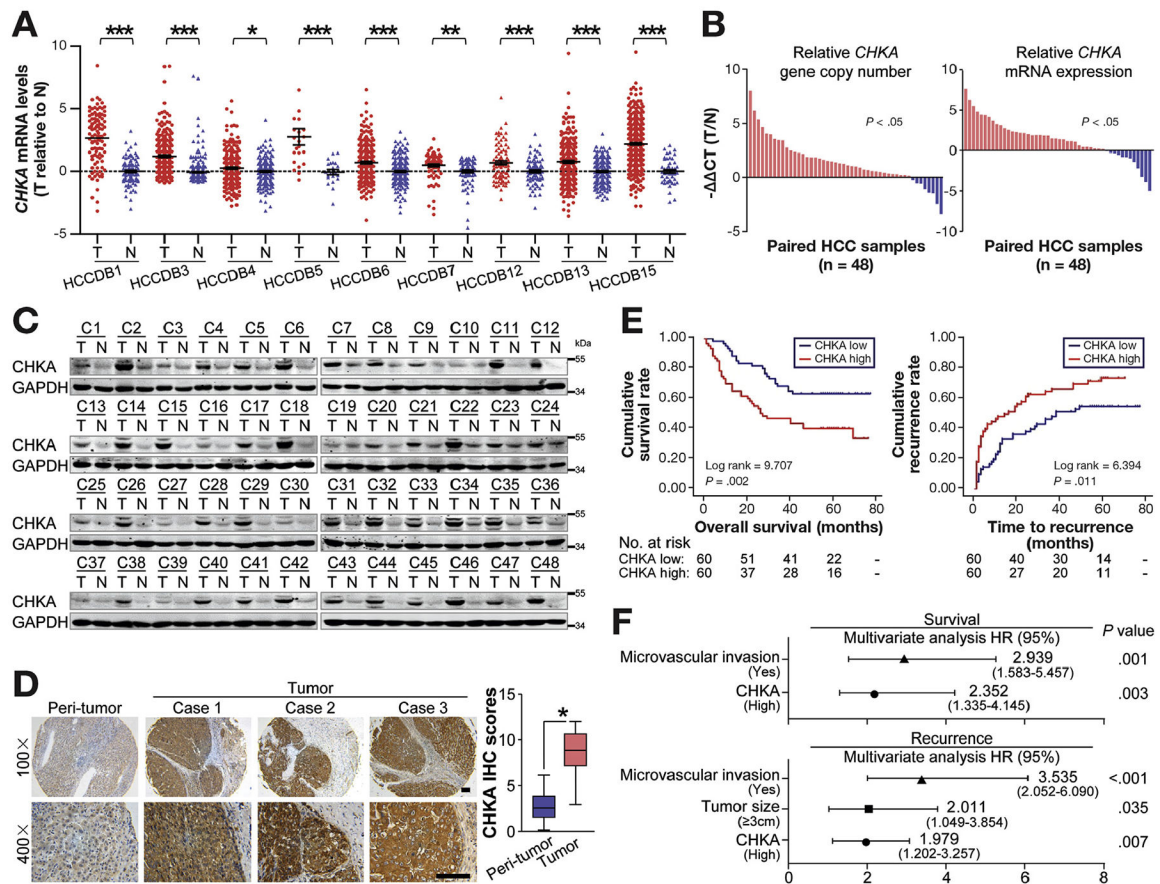
PI3K	phosphoinositide 3-kinase
mTORC2	mechanistic target of rapamycin complex 2
NC	negative control
RICTOR	RPTOR independent companion of mTOR complex 2
qRT-PCR	quantitative real-time polymerase chain reaction
sh	short hairpin
si	small interfering

References

1. Torre LA, Bray F, Siegel RL, et al. Global cancer statistics, 2012. *CA Cancer J Clin* 2015;65:87–108. [PubMed: 25651787]
2. El-Serag HB. Hepatocellular carcinoma. *N Engl J Med* 2011;365:1118–1127. [PubMed: 21992124]
3. Wang H, Chen L. Tumor microenvironment and hepato-cellular carcinoma metastasis. *J Gastroenterol Hepatol* 2013;28(Suppl 1):43–48. [PubMed: 23855295]
4. Li L, Tang J, Zhang B, et al. Epigenetic modification of MiR-429 promotes liver tumour-initiating cell properties by targeting Rb binding protein 4. *Gut* 2015;64:156–167. [PubMed: 24572141]
5. Hu L, Chen L, Li L, et al. Hepatitis B virus X protein enhances cisplatin-induced hepatotoxicity via a mechanism involving degradation of Mcl-1. *J Virol* 2011; 85:3214–3228. [PubMed: 21228225]
6. Buckley AF, Burgart LJ, Sahai V, et al. Epidermal growth factor receptor expression and gene copy number in conventional hepatocellular carcinoma. *Am J Clin Pathol* 2008;129:245–251. [PubMed: 18208805]
7. Whittaker S, Marais R, Zhu AX. The role of signaling pathways in the development and treatment of hepato-cellular carcinoma. *Oncogene* 2010;29:4989–5005. [PubMed: 20639898]
8. Mallarkey G, Coombes RC. Targeted therapies in medical oncology: successes, failures and next steps. *Ther Adv Med Oncol* 2013;5:5–16. [PubMed: 23323143]
9. Glunde K, Bhujwala ZM, Ronen SM. Choline metabolism in malignant transformation. *Nat Rev Cancer* 2011; 11:835–848. [PubMed: 22089420]
10. Aoyama C, Liao H, Ishidate K. Structure and function of choline kinase isoforms in mammalian cells. *Prog Lipid Res* 2004;43:266–281. [PubMed: 15003397]
11. Ramirez de Molina A, Rodriguez-Gonzalez A, Gutierrez R, et al. Overexpression of choline kinase is a frequent feature in human tumor-derived cell lines and in lung, prostate, and colorectal human cancers. *Biochem Biophys Res Commun* 2002;296:580–583. [PubMed: 12176020]
12. Ramirez de Molina A, Gutierrez R, Ramos MA, et al. Increased choline kinase activity in human breast carcinomas: clinical evidence for a potential novel antitumor strategy. *Oncogene* 2002;21:4317–4322. [PubMed: 12082619]
13. Glunde K, Raman V, Mori N, et al. RNA interference-mediated choline kinase suppression in breast cancer cells induces differentiation and reduces proliferation. *Cancer Res* 2005;65:11034–11043. [PubMed: 16322253]
14. Iorio E, Mezzanzanica D, Alberti P, et al. Alterations of choline phospholipid metabolism in ovarian tumor progression. *Cancer Res* 2005;65:9369–9376. [PubMed: 16230400]
15. Hernando E, Sarmentero-Estrada J, Koppie T, et al. A critical role for choline kinase- α in the aggressiveness of bladder carcinomas. *Oncogene* 2009; 28:2425–2435. [PubMed: 19448670]
16. Iorio E, Ricci A, Bagnoli M, et al. Activation of phosphatidylcholine cycle enzymes in human epithelial ovarian cancer cells. *Cancer Res* 2010;70:2126–2135. [PubMed: 20179205]
17. Trousil S, Lee P, Pinato DJ, et al. Alterations of choline phospholipid metabolism in endometrial cancer are caused by choline kinase α overexpression and a hyperactivated deacylation pathway. *Cancer Res* 2014; 74:6867–6877. [PubMed: 25267063]

18. Ramirez de Molina A, Gallego-Ortega D, Sarmentero J, et al. Choline kinase is a novel oncogene that potentiates RhoA-induced carcinogenesis. *Cancer Res* 2005; 65:5647–5653. [PubMed: 15994937]
19. Asim M, Massie CE, Orafidiya F, et al. Choline kinase alpha as an androgen receptor chaperone and prostate cancer therapeutic target. *J Natl Cancer Inst* 2016; 108(5):djv371.
20. Granata A, Nicoletti R, Tinaglia V, et al. Choline kinase-alpha by regulating cell aggressiveness and drug sensitivity is a potential druggable target for ovarian cancer. *Br J Cancer* 2014;110:330–340. [PubMed: 24281000]
21. Ramirez de Molina A, Sarmentero-Estrada J, Belda-Iniesta C, et al. Expression of choline kinase alpha to predict outcome in patients with early-stage non-small-cell lung cancer: a retrospective study. *Lancet Oncol* 2007;8:889–897. [PubMed: 17851129]
22. Miyake T, Parsons SJ. Functional interactions between choline kinase alpha, epidermal growth factor receptor and c-Src in breast cancer cell proliferation. *Oncogene* 2012;31:1431–1441. [PubMed: 21822308]
23. Wu X, Jiang R, Zhang MQ, et al. Network-based global inference of human disease genes. *Mol Syst Biol* 2008;4.
24. Chua BT, Gallego-Ortega D, Ramirez de Molina A, et al. Regulation of Akt(ser473) phosphorylation by choline kinase in breast carcinoma cells. *Mol Cancer* 2009;8:131. [PubMed: 20042122]
25. Yalcin A, Clem B, Makoni S, et al. Selective inhibition of choline kinase simultaneously attenuates MAPK and PI3K/AKT signaling. *Oncogene* 2010;29:139–149. [PubMed: 19855431]
26. Yan HX, Wang HY, Zhang R, et al. Negative regulation of hepatocellular carcinoma cell growth by signal regulatory protein alpha1. *Hepatology* 2004;40:618–628. [PubMed: 15349900]
27. Sorokin A, Lemmon MA, Ullrich A, et al. Stabilization of an active dimeric form of the epidermal growth factor receptor by introduction of an inter-receptor disulfide bond. *J Biol Chem* 1994;269:9752–9759. [PubMed: 8144568]
28. Sarbassov DD, Guertin DA, Ali SM, et al. Phosphorylation and regulation of Akt/PKB by the rictor-mTOR complex. *Science* 2005;307:1098–1101. [PubMed: 15718470]
29. Feldman ME, Apsel B, Uotila A, et al. Active-site inhibitors of mTOR target rapamycin-resistant outputs of mTORC1 and mTORC2. *PLoS Biol* 2009;7:e38. [PubMed: 19209957]
30. Prahallad A, Sun C, Huang S, Di Nicolantonio F, et al. Unresponsiveness of colon cancer to BRAF(V600E) inhibition through feedback activation of EGFR. *Nature* 2012;483:100–103. [PubMed: 22281684]
31. Braconi C, Meng F, Swenson E, et al. Candidate therapeutic agents for hepatocellular cancer can be identified from phenotype-associated gene expression signatures. *Cancer* 2009;115:3738–3748. [PubMed: 19514085]
32. Sawey ET, Chanrion M, Cai C, et al. Identification of a therapeutic strategy targeting amplified FGF19 in liver cancer by oncogenomic screening. *Cancer Cell* 2011; 19:347–358. [PubMed: 21397858]
33. Glunde K, Shah T, Winnard PT Jr, et al. Hypoxia regulates choline kinase expression through hypoxia-inducible factor-1 alpha signaling in a human prostate cancer model. *Cancer Res* 2008;68:172–180. [PubMed: 18172309]
34. Belouèche-Babari M, Arunan V, Troy H, et al. Histone deacetylase inhibition increases levels of choline kinase alpha and phosphocholine facilitating noninvasive imaging in human cancers. *Cancer Res* 2012;72: 990–1000. [PubMed: 22194463]
35. Ward CS, Eriksson P, Izquierdo-Garcia JL, et al. HDAC inhibition induces increased choline uptake and elevated phosphocholine levels in MCF7 breast cancer cells. *PLoS One* 2013;8:e62610. [PubMed: 23626839]
36. Ling CS, Yin KB, Cun ST, et al. Expression profiling of choline and ethanolamine kinases in MCF7, HCT116 and HepG2 cells, and the transcriptional regulation by epigenetic modification. *Mol Med Rep* 2015;11: 611–618. [PubMed: 25333818]
37. Domizi P, Aoyama C, Banchio C. Choline kinase alpha expression during RA-induced neuronal differentiation: role of C/EBPbeta. *Biochim Biophys Acta* 2014; 1841:544–551. [PubMed: 24440820]

38. Al-Saffar NM, Jackson LE, Raynaud FI, et al. The phosphoinositide 3-kinase inhibitor PI-103 downregulates choline kinase alpha leading to phosphocholine and total choline decrease detected by magnetic resonance spectroscopy. *Cancer Res* 2010;70:5507–5517. [PubMed: 20551061]
39. Wang RY, Chen L, Chen HY, et al. MUC15 inhibits dimerization of EGFR and PI3K-AKT signaling and is associated with aggressive hepatocellular carcinomas in patients. *Gastroenterology* 2013;145:1436–1448 e1–12. [PubMed: 23933603]
40. Jiang F, Chen L, Yang YC, et al. CYP3A5 functions as a tumor suppressor in hepatocellular carcinoma by regulating mTORC2/Akt signaling. *Cancer Res* 2015; 75:1470–1481. [PubMed: 25649767]
41. Clem BF, Clem AL, Yalcin A, et al. A novel small molecule antagonist of choline kinase-alpha that simultaneously suppresses MAPK and PI3K/AKT signaling. *Oncogene* 2011;30:3370–3380. [PubMed: 21423211]
42. Falcon SC, Hudson CS, Huang Y, et al. A non-catalytic role of choline kinase alpha is important in promoting cancer cell survival. *Oncogenesis* 2013;2.

**Figure 1.**

Increased CHKA expression correlates with aggressive clinicopathologic features and predicts poor prognosis in HCC patients. (A) The gene chip data were obtained from 9 HCC databases. Relative expression levels of *CHKA* messenger RNA (mRNA) in HCC and adjacent nontumor tissues were shown. * $P < .05$; ** $P < .01$; *** $P < .001$, based on Student *t* test. (B) The relative levels of *CHKA* copy number (left) and *CHKA* mRNA (right) in 48 paired HCC and adjacent nontumor tissues were evaluated by qRT-PCR. (C) Western blots showing the expression of the *CHKA* protein in 48 paired HCC and adjacent nontumor tissues. Glyceraldehyde-3-phosphate dehydrogenase (GAPDH) was used as a loading control. (D) Immunohisto-chemistry (IHC) of *CHKA* on tissue microarrays containing 120 paired HCC and adjacent nontumor tissues. Images of representative staining are shown. Scale bar = 100 μ m. Relative IHC scores were shown as mean \pm SD, * $P < .05$, based on the Wilcoxon matched pairs test. (E) The cumulative survival and cumulative recurrence for the low and high *CHKA* expression groups of the 120 HCC patients were significantly different (by the 2-sided log-rank test). The absolute number of patients at risk is listed below each curve. (F) A multivariate analysis of the hazard ratios (HRs) showed that the up-regulation of *CHKA* may be an independent prognostic factor for overall survival and recurrence-free survival rates (by the Cox multivariate proportional hazard regression model). The HRs are presented as the mean (95% confidence interval). The variables included in the multivariate analysis were selected using a univariate analysis.

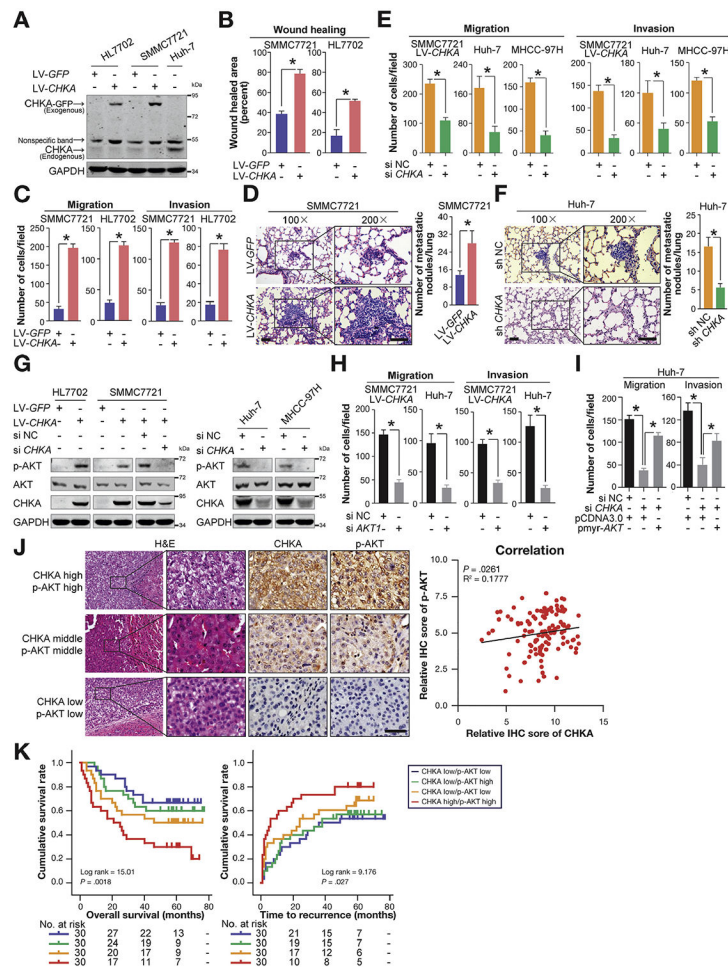


Figure 2. CHKA enhances invasion and metastasis of HCC cells via activating AKT. (A) The GFP-tagged *CHKA* stably transfected HL7702 and SMMC7721 cell lines and their control cell lines were established using lentivirus. The exogenous GFP-tagged CHKA protein and endogenous CHKA protein in the stably transfected cell lines and the Huh-7 cell line were detected by Western blots. Glyceraldehyde-3-phosphate dehydrogenase (GAPDH) was used as a loading control. (B) Scratch wound healing assays were performed using the indicated cell lines. Results are shown as mean \pm SD (n = 3). * P < .05, based on Student t test. (C) Migration and invasion assays were used to test the migration and invasion abilities of the indicated cell lines. Results are shown as mean \pm SD (n = 3). * P < .05, based on Student t test. (D) Representative lung tissue sections of BALB/C nude mice killed at 8 weeks from each group are shown (H&E; scale bar = 100 μ m). The mean number of lung metastatic tumors per lung in each group was calculated. Results are shown as mean \pm SD (n = 5). * P < .05, based on Student t test. (E) Migration and invasion assays were performed 48 hours after the indicated cell lines treated with 100 nM *CHKA* siRNA (si*CHKA*) or siRNA-negative control (siNC). Results are shown as mean \pm SD (n = 3). * P < .05, based on Student t test. (F) Representative lung tissue sections of BALB/C mice killed at 8 weeks from each group are shown (H&E; scale bar = 100 μ m). Mean number of lung metastatic tumors per lung in each group was calculated. Results are shown as mean \pm SD (n = 5). * P < .05, based

on the Student *t* test. (*G*) The background total expression levels and phosphorylation levels of AKT (p-AKT) were analyzed by Western blotting in the indicated cell lysates. GAPDH was used as a loading control. (*H*) Migration and invasion assays were performed 48 hours after the indicated cell lines were treated with 100 nM *AKT1* siRNA (si*AKT1*) or siNC. Results are shown as mean \pm SD (n = 3). **P* < .05, based on Student *t* test. (*I*) Huh-7 cells were transiently transfected with 100 nM si*CHKA* or siNC, a control vector (pCDNA3.0) or pmyr-*AKT*. Forty-eight hours post transfection, cells were subjected to migration assays or invasion assays. Results are shown as mean \pm SD (n = 3). **P* < .05, based on the 1-way analysis of variance. (*J*) Correlation between CHKA and p-AKT expression level was examined among 120 patients as assessed by tissue microarray, $R^2 = 0.1777$; *P* = .0261 by Spearman's nonparametric correlation test. Representative immunohistochemical (IHC) staining of CHKA and p-AKT in serial sections were shown on the *left*, showing the positive correlation between the level of CHKA and that of p-AKT in the clinical samples. (*K*) The combination of CHKA and p-AKT increased the probability of a poor prognosis (by the 2-sided log-rank test). The absolute number of patients at risk is listed *below each curve*.

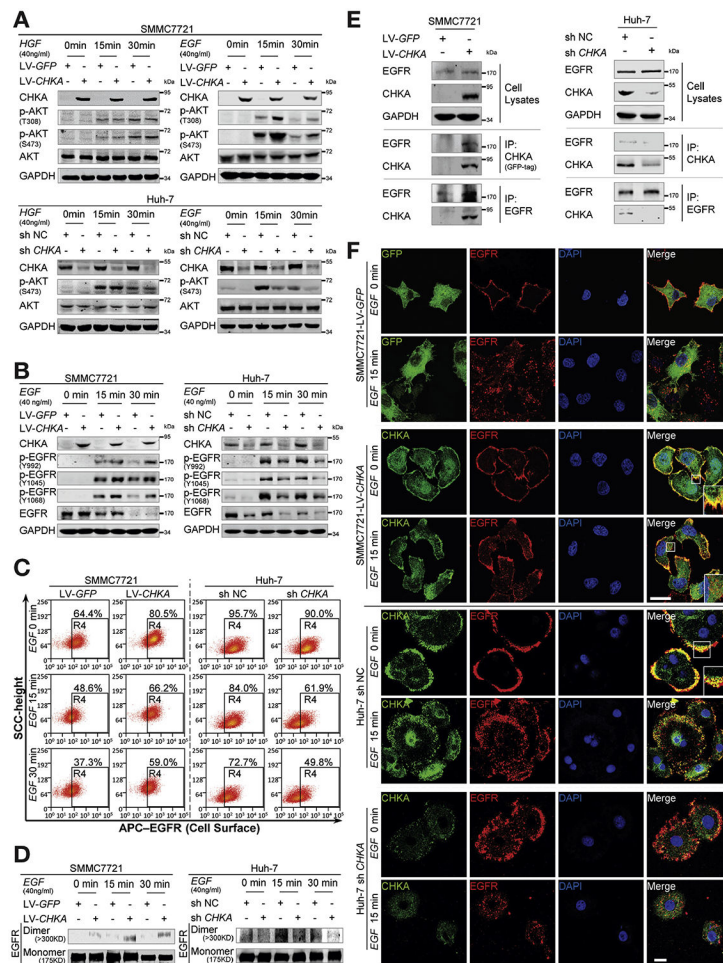


Figure 3. CHKA physically interacts with EGFR and promotes EGFR autophosphorylation and dimerization on plasma membrane. (A) After being starved with serum-free Dulbecco's modified Eagle medium (DMEM) for 16 hours, the indicated cell lines were exposed to EGF or hepatocyte growth factor (HGF) for 0, 15, or 30 minutes and analyzed by Western blotting with indicated antibodies. Glyceraldehyde-3-phosphate dehydrogenase (GAPDH) was used as a loading control. (B) After being starved with serum-free DMEM for 16 hours, the indicated cell lines were exposed to EGF for 0, 15, or 30 minutes and analyzed by Western blotting with indicated antibodies. GAPDH was used as a loading control. (C) The cell surface expression levels of EGFR in the indicated cells were determined using flow cytometry. (D) The indicated cells were stimulated with EGF for 0, 15, or 30 minutes and incubated on ice for 30 minutes with the cross-linking reagent bis (sulfosuccinimidyl) substrate (3 mM). Cell lysates were subjected to Western blot assays. Dimers were visualized as >300-kD bands, with monomers serving as loading controls. (E) The indicated cell lysates were prepared and immunoprecipitated (IP) with either agarose-conjugated anti-EGFR, anti-GFP (for GFP-tagged CHKA), or anti-CHKA (for endogenous CHKA) antibodies. Immunoprecipitates and cell lysates were analyzed by Western blotting. (F) The CHKA overexpressed SMMC7721 cell line and its control cell line, and the CHKA depleted Huh-7 cell line and its control cell line were stimulated with EGF for 0 or 15 minutes,

followed by immunofluorescence assays. The localizations of EGFR and GFP-fused CHKA or GFP alone (in SMMC7721), and the localizations of EGFR and endogenous CHKA (in Huh-7) were detected by confocal laser scanning microscopy as indicated. Scale bar = 20 μm .

Author Manuscript

Author Manuscript

Author Manuscript

Author Manuscript

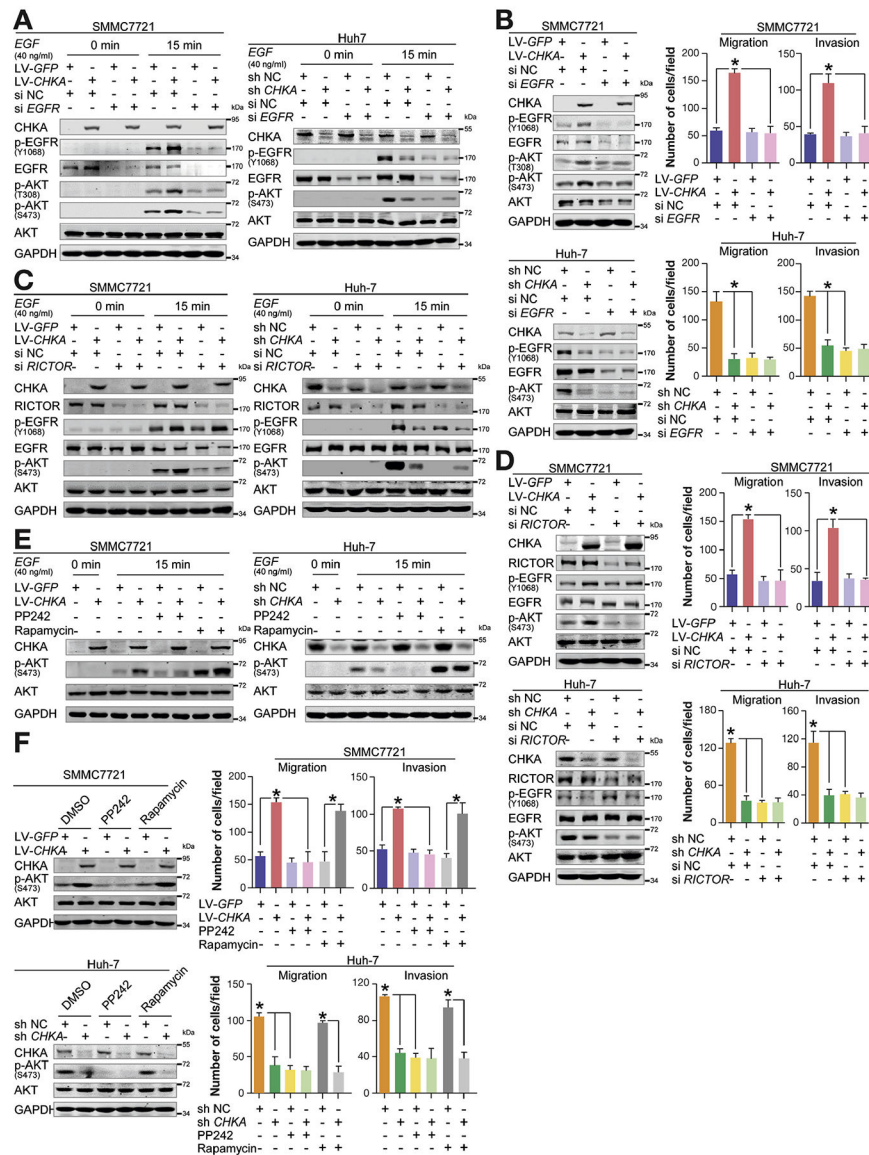


Figure 4. EGFR-mTORC2 axis is indispensable for CHKA-induced AKT activation and HCC metastasis. (A) Thirty-two hours after transfection with 100 nM siRNA of *EGFR* (si*EGFR*) or negative control (siNC), the indicated cell lines were starved with serum-free Dulbecco’s modified Eagle medium (DMEM) for 16 hours, and then exposed to EGF for 0 or 15 minutes, followed by Western blotting with the indicated antibodies. Glyceraldehyde-3-phosphate dehydrogenase (GAPDH) was used as a loading control. (B) Forty-eight hours after transfection with 100 nM si*EGFR* or siNC, the indicated cells were analyzed by Western blotting with the indicated antibodies (*left*). GAPDH was used as a loading control. The motility abilities of the indicated cells after treatments were also analyzed using the migration and invasion assays (*right*). Results are shown as mean \pm SD (n = 3). **P* < .05, based on the 1-way analysis of variance (ANOVA). (C) Thirty-two hours after transfection with 100 nM siRNA of *RICTOR* (si*RICTOR*) or negative control, the indicated cell lines

were starved with serum-free DMEM for 16 hours, and then were exposed to EGF for 0 or 15 minutes, followed by Western blotting with the indicated antibodies. GAPDH was used as a loading control. (D) Forty-eight hours after transfection with 100 nM si*RICTOR* or siNC, the indicated cells were analyzed by Western blotting with the indicated antibodies (*left*). GAPDH was used as a loading control. The motility abilities of the indicated cells after treatments were also analyzed using the migration and invasion assays (*right*). Results are shown as mean \pm SD (n = 3). **P* < .05, based on the 1-way ANOVA. (E) The indicated cells were first starved and then pretreated with inhibitors for 6 hours, exposed to EGF for 15 minutes, and analyzed by Western blotting with the indicated antibodies. GAPDH was used as a loading control. PP242 (2 μ M), mTORC1/C2 inhibitor; rapamycin (10 nM), mTORC1 inhibitor. (F) Western-blot analysis of the effect of the drugs on the indicated cell lines treated with various inhibitors or dimethyl sulfoxide (*left*). PP242 (2 μ M); rapamycin (10 nM). GAPDH was used as a loading control. The motility abilities of the indicated cells after treatments were also analyzed using the migration and invasion assays (*right*). Results were shown as mean \pm SD (n = 3). **P* < .05, based on the 1-way ANOVA.

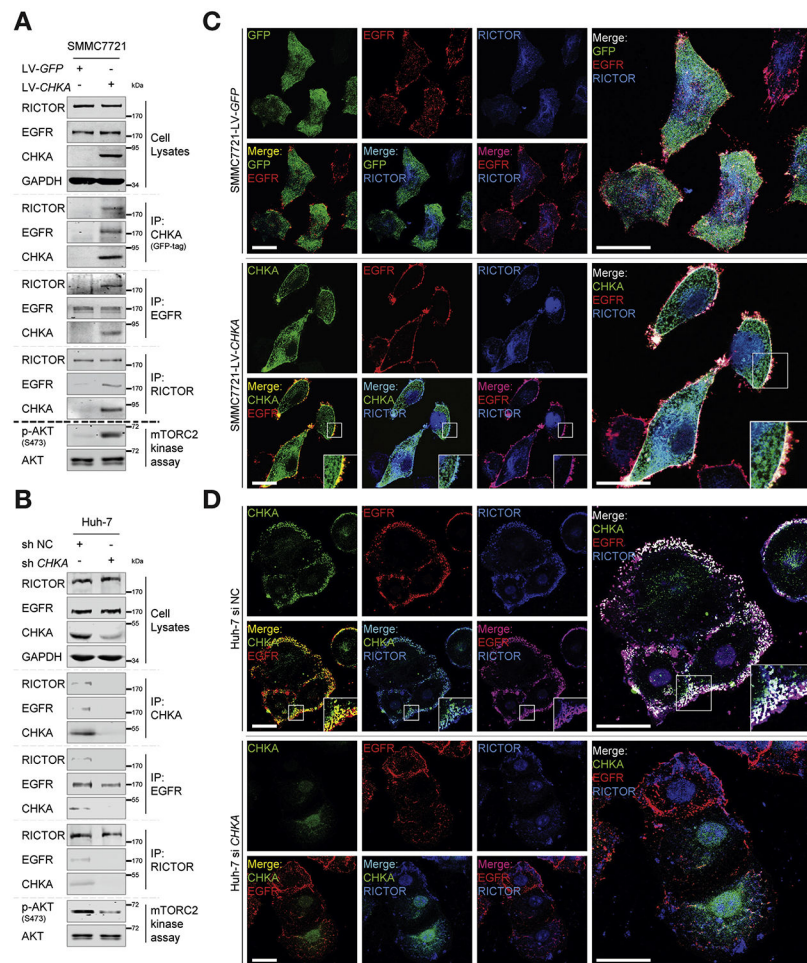


Figure 5. CHKA acts as an adaptor protein tethering EGFR and RICTOR. (A, B) The indicated cell lysates were prepared and immunoprecipitated with either agarose-conjugated anti-EGFR, anti-RICTOR, anti-GFP (for GFP-tagged CHKA), or anti-CHKA (for endogenous CHKA) antibodies, followed by mTORC2 kinase activity assay. Immunoprecipitates and cell lysates were analyzed by Western blotting. (C) Immunofluorescence assays were performed using the CHKA overexpressed SMMC7721 cell line and its control cell line. The localizations of RICTOR, EGFR, and GFP-tagged CHKA or GFP alone were detected by confocal laser scanning microscopy as indicated. Scale bar = 20 μ m. (D) Immunofluorescence assays were performed after Huh-7 cells were transfected with 100 nM siCHKA or siNC for 48 hours. The localizations of EGFR, RICTOR, and CHKA were detected by confocal laser scanning microscopy as indicated. Scale bar = 20 μ m.

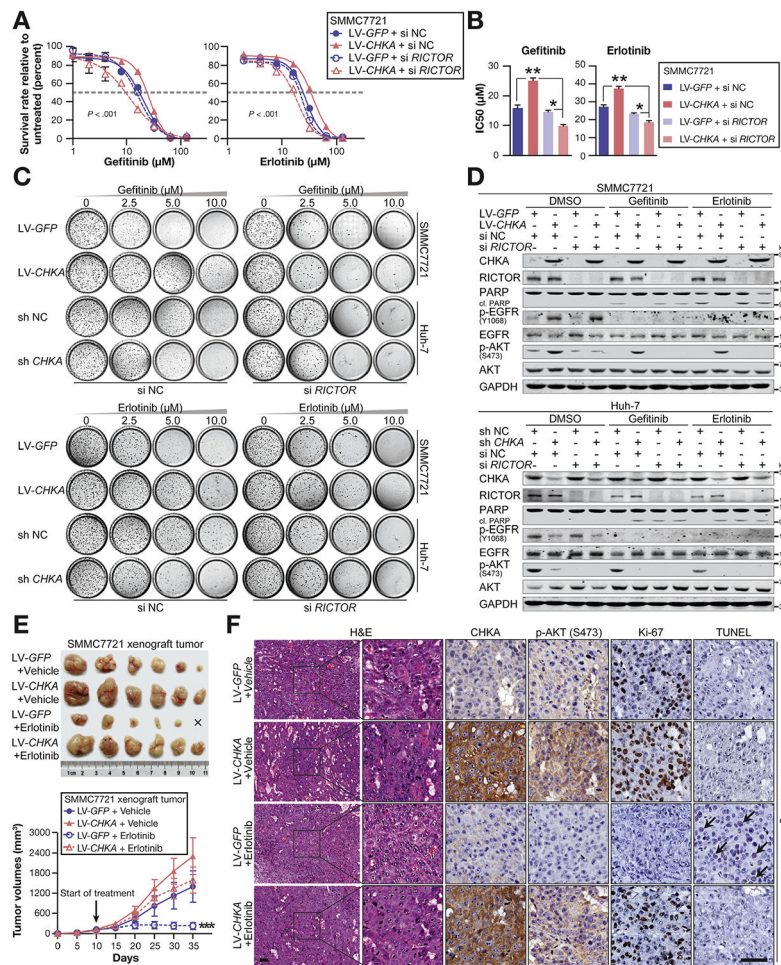


Figure 6. Overexpression of CHKA promotes resistance to anti-EGFR drugs in HCC. (A, B) Short-term growth-inhibition assays of the indicated cell lines. Cells were treated with increasing concentrations of EGFR inhibitors, gefitinib or erlotinib, for 72 hours, and cell viability was determined using CCK8 by measuring the absorbance at 450 nm in a microplate reader. (A) Survival rate (relative to untreated cells) were shown as mean \pm SD (n = 3); * P < .001, based on the 2-way analysis of variance (ANOVA), and (B) 50% inhibitory concentration (IC₅₀) values were calculated through nonlinear regression fit curve analysis and were shown as mean \pm SD (n = 3); * P < .05, based on the 1-way ANOVA. (C) Long-term colony-formation assay of the indicated cell lines. Cells were grown in the absence or presence of gefitinib or erlotinib at the indicated concentrations for 10–14 days. For each cell line, all dishes were fixed at the same time, stained, and photographed. (D) Western-blot analysis of the effect of the drugs on the indicated cell lines treated with various inhibitors. Gefitinib (10 μ M), erlotinib (10 μ M). Glyceraldehyde-3-phosphate dehydrogenase (GAPDH) was used as a loading control. (E, F) In vivo xenograft tumor-formation assays were performed using LV-GFP or LV-CHKA stably transfected SMMC7721 cells (1×10^6) subcutaneously injected into the right posterior flanks of 6-week-old female BALB/C nude mice, followed by treatment with vehicle or erlotinib (80 mg/kg/d) when the tumor reached a volume of approximately 100 mm³ in size. Tumor growth was measured every 5 days. At day 40, mice

were sacrificed and tumors were photographed. Results were shown as mean \pm SD (n = 6); *** $P < .001$, based on the 2-way ANOVA. (F) H&E, immunohistochemical (CHKA, p-AKT, Ki-67), and terminal deoxynucleotidyl transferase-mediated deoxyuridine triphosphate nick-end labeling staining were performed on paraffin-embedded specimens of xenograft tumors.

Author Manuscript

Author Manuscript

Author Manuscript

Author Manuscript

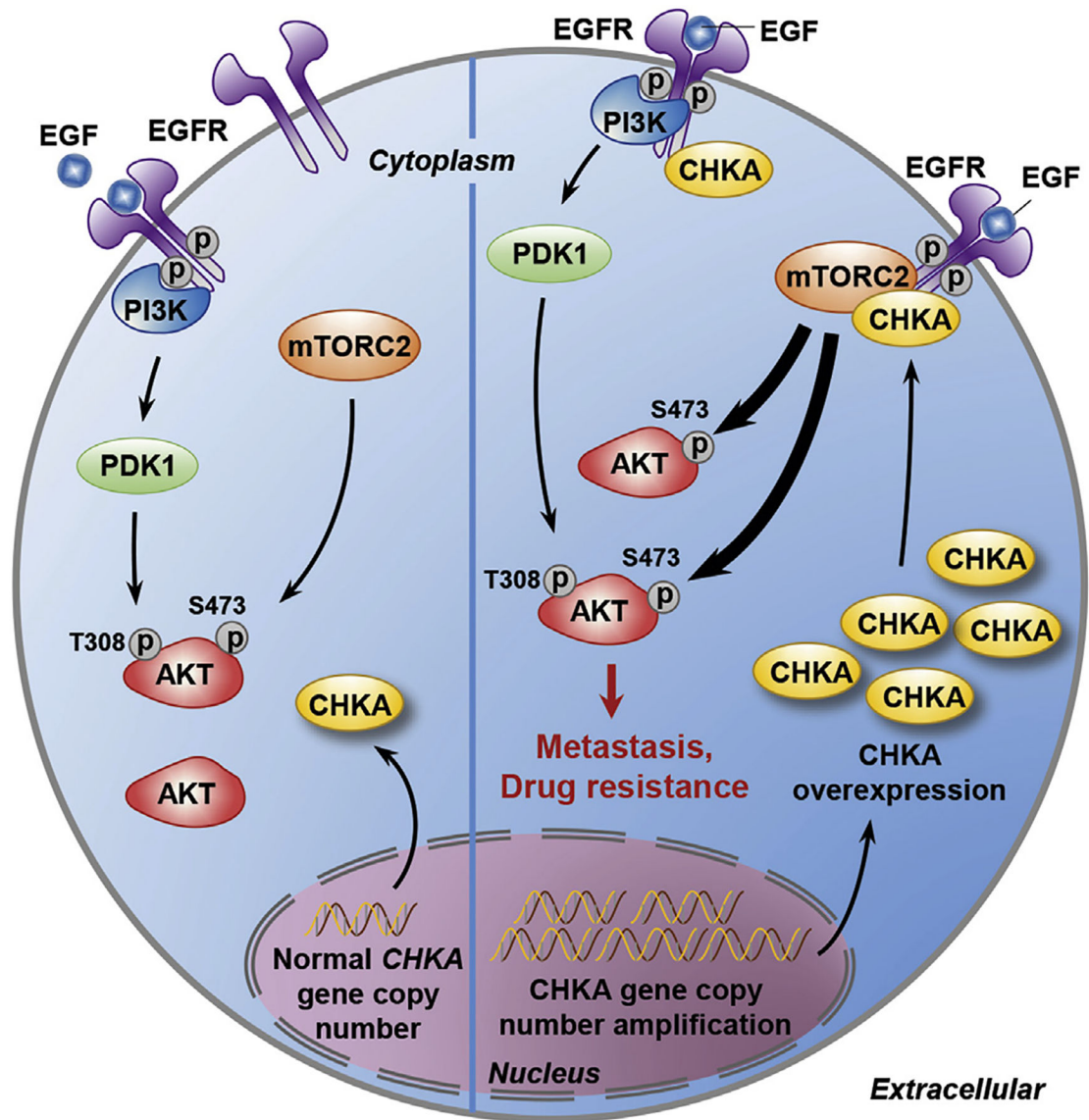


Figure 7. Schematic depiction of the mechanisms underlying CHKA-mediated HCC metastasis and drug resistance via tethering EGFR and mTORC2 for AKT activation.